Supplemental Information for

Brown Carbon in Primary and Aged Coal Combustion Emission

Haiyan Ni,[†,‡] Ru-Jin Huang,[,†,∥] Simone M. Pieber,[§,**] Joel C. Corbin,[§,***] Giulia Stefenelli,[§] Veronika Pospisilova,[§] Felix Klein,[§,****] Martin Gysel-Beer,[§] Lu Yang,[†] Urs Baltensperger,[§] Imad El Haddad,[§] Jay G. Slowik,[§] Junji Cao,[†] André S. H. Prévôt,[§] Ulrike Dusek [‡]*

[†]State Key Laboratory of Loess and Quaternary Geology, Key Laboratory of Aerosol Chemistry and Physics, CAS Center for Excellence in Quaternary Science and Global Change, Institute of Earth Environment, Chinese Academy of Sciences, Xi'an 710061, China

[‡]Centre for Isotope Research (CIO), Energy and Sustainability Research Institute Groningen (ESRIG), University of Groningen, the Netherlands

[§]Laboratory of Atmospheric Chemistry, Paul Scherrer Institute (PSI), Villigen, 5232, Switzerland

[∥]Institute of Global Environmental Change, Xi'an Jiaotong University, Xi'an, 710049, China

[**]Now at: Laboratory for Air Pollution / Environmental Technology, Empa, Ueberlandstrasse 129, CH-8600 Duebendorf, Switzerland

[***]Now at: Metrology Research Centre, National Research Council Canada, Ottawa K1A 0R6, Ontario, Canada

[****]Now at: Meteorologisches Observatorium Hohenpeissenberg, Deutscher Wetterdienst (DWD), Hohenpeissenberg 82383, Germany

*Corresponding author: rujin.huang@ieecas.cn

Summary

Number of pages: 15

Number of texts: 6

Number of figures: 6

Number of tables: 4

Text S1. Coal, burner and burning procedure

Coal and burner Coals used in this study are classified into anthracite coal and bituminous coal based on their volatile matter content (V_{daf}). According to the national standards of the People's Republic of China (GB/T 5751-2009), V_{daf} for anthracite coal is less than or equal to 10 % ($V_{daf} \leq 10$ %), whereas bituminous coal has higher V_{daf} (>10 %). The V_{daf} of coals was measured by Shaanxi Coal Geological Laboratory Co., Ltd., China on the basis of the national standards (GB/T 212-2008) and was shown in Table S1. All collected coals were stored at ambient temperature and humidity before the experiments.

The stove was purchased from a local market and is one of most widely used stoves in residential households in northern China for cooking and heating, especially for families without central heating system. The stove has a metallic outer cover and thermal-insulated ceramic liner, and an iron grate inside separating burning zone and ash. It was 51 cm in height, 31 cm in outer diameter and 12 cm in inner diameter. There was a 6 cm diameter air-control hole in the outer cover near the bottom, which was fully open to let in air during combustion in this campaign.

Coal combustion procedure A hot honeycomb and anthracite coal (fairly clean fuel[1]) was used to pre-heat the stove until the temperature above the coal bed reaches ~650 ºC. Temperature in the combustion chamber of the stove was monitored with a thermocouple probe situated closely above the coal. Then 200–300 g coal was put in the stove to begin the coal combustion experiment.

Text S2. Smog chamber

The PSI smog chamber used in this study has been described in details elsewhere.[2-5] In brief, it is a 7 m^3 Teflon bag made of a 125 μm thick Teflon foil, and seats in a temperature-controlled trailer. A set of UV lights (40 × 90–100 W, Cleo Performance, Philips) is installed to initiate photooxidation of the emissions. At the start of each experiment the smog chamber was filled to approximately two thirds full with humidified air, leaving a volume free for sample injection. After injection (which typically lasted for 30–50 min), the chamber volume was filled up to its maximum, and the relative humidity (RH) was adjusted to 50 %. After each experiment, the chamber was cleaned by injecting O_3 until the concentration of O_3 up to 2 ppm and irradiating with a set of UV lights for at least 2 h,

while flushing with zero air. The chamber was then flushed with pure air in the dark overnight (roughly 12 h). After cleaning, the chamber was partially filled with humidified pure air. Background measurements of the clean chamber were conducted prior to each experiment.

Text S3. Equivalent black carbon (eBC) measurement

eBC measurements were conducted with an Aethalometer (Model AE33, Magee Scientific). The newly developed model AE33 uses the DualSpot Technology® for real-time loading compensation.[6] From the change in optical attenuation at 880 nm measured by the Aethalometer and using the mass absorption cross section of 7.77 m^2 g^{-1}, eBC concentrations were retrieved. At 880 nm, the light absorption can be attributed to BC alone, because other particles (e.g., mineral) absorb significantly less.

Text S4. UV–visible absorbance measurements

Two punches (10 mm diameter) from each filter sample were used for the UV–visible absorbance measurements. One punch was extracted in 3 mL ultrapure water (Millipore synergy UV) under 25 min sonication at 30 °C, and the other was extracted in 3 mL methanol (Sigma, chromatographic grade). The extracts were subsequently vortexed for 1 min and then filtered with 0.45 μm nylon filters to remove particles in suspension.[7]

Light absorption spectra of the extracts were measured over the wavelength range of 280–500 nm using a UV–visible spectrophotometer (Ocean Optics) coupled to a 50 cm long-path detection cell.[8-10] Absorption spectra were recorded using OceanView software (Ocean Optics). The spectrometer measures the optical attenuation (ATN) by the OA in the extracts. ATN at a given wavelength λ (ATN_λ) of the solution, recorded as the logarithm of the ratio of signal intensities of the reference (solvent) (I_0) and the sample (I), both corrected for background signals with the light source off, can be converted to the absorption coefficient of solutions at λ ($b_{abs,\lambda}$ in Mm^{-1}) by:

$$b_{\mathrm{abs},\lambda} = \mathrm{ATN}_\lambda \times \frac{V_{\mathrm{solution}}}{V_{\mathrm{air}} \times l} \times \ln 10 \qquad \text{(S1)}$$

where $V_{solution}$ (mL) is the solution volume that the filter punch is extracted into. V_{air} (m^3) is the air volume sampled through the filter punch. ATN_λ is already corrected for baseline drift, while ln10 converts from common logarithm to natural logarithm, the form in which

atmospheric measurements are typically reported. l (m) is the absorbing path length. A blank correction was performed for b_{abs} by subtracting the averaged b_{abs} of the blank filters including filters collected from the cleaned chamber before injection and from the control experiments (i.e., experiments performed analogous to the aging of emissions, but without actually injecting emissions in the smog chamber) (Figures S3, S4; Table S2).

Text S5. Uncertainties of MAE

The uncertainties of measured MAE, δ(MAE), can be derived from:

$$\delta(\mathrm{MAE}) = \mathrm{MAE} \times \sqrt{\left(\frac{\delta(b_{\mathrm{abs}})}{b_{\mathrm{abs}}}\right)^2 + \left(\frac{\delta(C_{\mathrm{OA}})}{C_{\mathrm{OA}}}\right)^2} \quad \text{(S2)}$$

where C_{OA} with uncertainties $\delta(C_{OA})$ are given in Table S3; b_{abs} is blank corrected, thus uncertainties of b_{abs} is:

$$\delta(b_{\mathrm{abs}}) = \sqrt{(\delta(b_{\mathrm{abs\_raw}}))^2 + (\delta(b_{\mathrm{abs\_blank}}))^2} \quad \text{(S3)}$$

where $b_{\mathrm{abs\_raw}}$ is the raw b_{abs} without blank correction, and $b_{\mathrm{abs\_blank}}$ is the b_{abs} of the blank filters. Standard deviation (SD) of average b_{abs_blank} for blank filters (Figure S4) is used to represent $\delta(b_{abs-blank})$. For $\delta(b_{abs-raw})$, both noise and precision of the instrument are considered following the method of Rocke and Lorenzato[11] and Wilson et al.[12]. The error introduced by the instrument noise is assumed to be equal to the $\delta(b_{abs-blank})$, because the noise is more representative of error for low signal measurements. To provide the overall $\delta(b_{abs-raw})$, the uncertainties from noise (= $\delta(b_{abs-blank})$) and prevision (10%) of the instrument were added in quadrature.

Table S3 shows the MAE_{365} of the methanol extracts with their uncertainties. The uncertainties mainly come from the blank correction. Thus, for sample whose signal is closer to averaged blank signal, the uncertainty is larger.

Text S6. Sensitivity of POA(t) on the SOA(t)/OA(t) and MAE_{SOA}

In our study, we assume that changes of POA concentration are exclusively due to wall losses (eq 5) during the smog chamber experiment. However, a fraction of POA can be volatilized and oxidized during aging, which is not considered in our analysis and thus possibly affects the calculation of SOA(t)/OA(t) and MAE_{SOA} following eqs 6–7. To address this concern, we employ a sensitivity analysis. If the POA(t) decreases by 20% due

to the aging of POA during the smog chamber experiments, the average mass ratios of SOA(t)/OA(t) change by less than 4% (Figure S6). The small change of SOA(t)/OA(t) further translates into an increase of the derived MAE_{365} of SOA following eq 6 from 0.14 ± 0.08 m^2 g^{-1} to 0.16 ± 0.11 m^2 g^{-1} (Figure S6). This change of MAE_{365} of SOA is also small, which is consistent with our expectation, because SOA dominates the aged OA mass (i.e., high SOA(t)/OA(t) ratios as shown in Figure 5a). Therefore, a moderate loss of POA will not change our conclusion that the estimated MAE_{365} of SOA was much lower than that of POA (0.84 ± 0.54 m^2 g^{-1}).

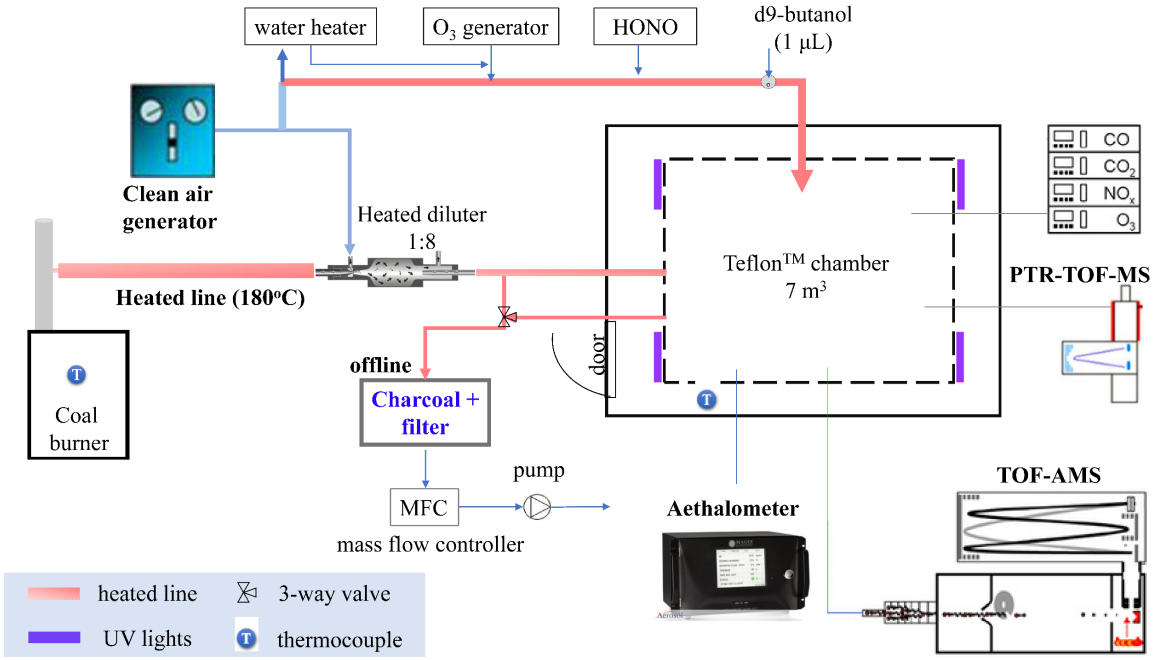

Figure S1. Schematic of the smog chamber setup for coal combustion experiments. The coals were burned in the stove, and the emissions were sampled from the chimney, diluted by the dilutor, and then injected into the smog chamber. After injection, primary emissions in the chamber were collected on a quartz fiber filter for offline UV–visible absorbance measurements. Then we injected butanol-D9, HONO, and turned on the UV lights, and started aging. After 2.5–5 h aging, aged particles were collected on another filter.

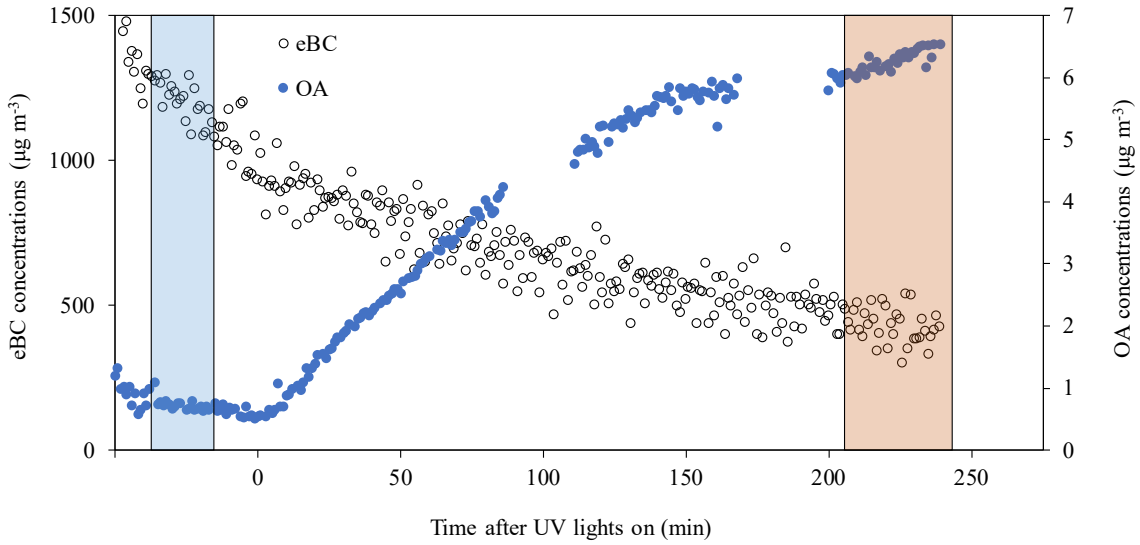

Figure S2. Equivalent black carbon (eBC) concentrations of primary and aged emissions measured at 880 nm using an Aethalometer in a typical combustion experiment of bituminous coal (coal B1; experiment B1-03, Table S2). The OA concentration was measured by a HR-ToF-AMS (Aerodyne Research Inc.). The highlighted boxes mark the time periods when the filter samples of primary and aged emissions were collected. Before lights on, the concentrations of eBC and OA decreased because of wall loss. After switching on the lights, the OA concentrations increased due to SOA formation.

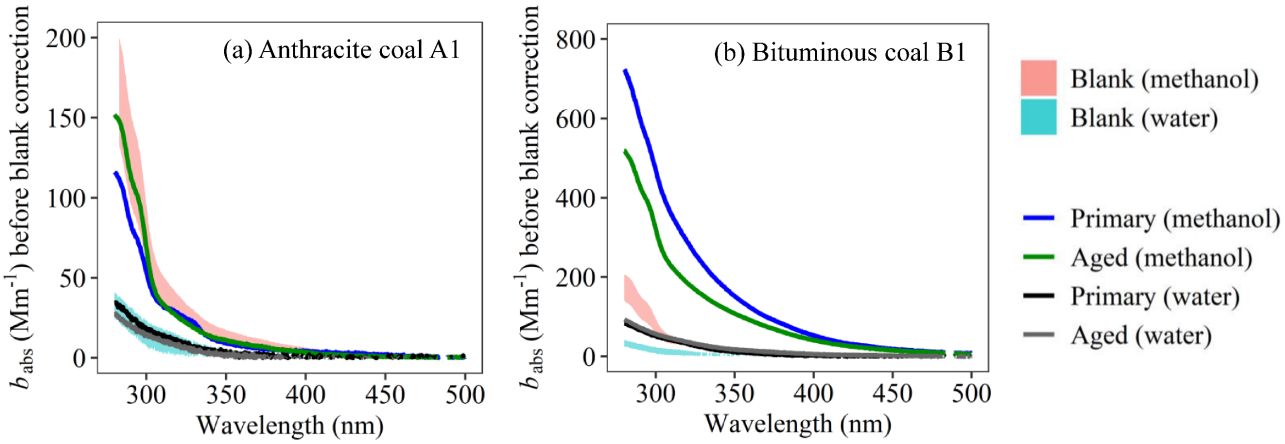

Figure S3. Example solution spectra of methanol and water extracts from the primary and aged samples of **(a)** anthracite coal A1 (experiment A1-16) and **(b)** bituminous coal B1 (experiment B1-01). For anthracite coal, the b_{abs} is below or very close to the b_{abs} of blanks. The blank-corrected b_{abs} for bituminous coal B1 is shown in Figure 1 in the main text. All the b_{abs} values (Mm^{-1}) are not wall loss corrected. b_{abs} had small variations for blank filters collected from the cleaned chamber and from the control experiments, as shown in Figure S4.

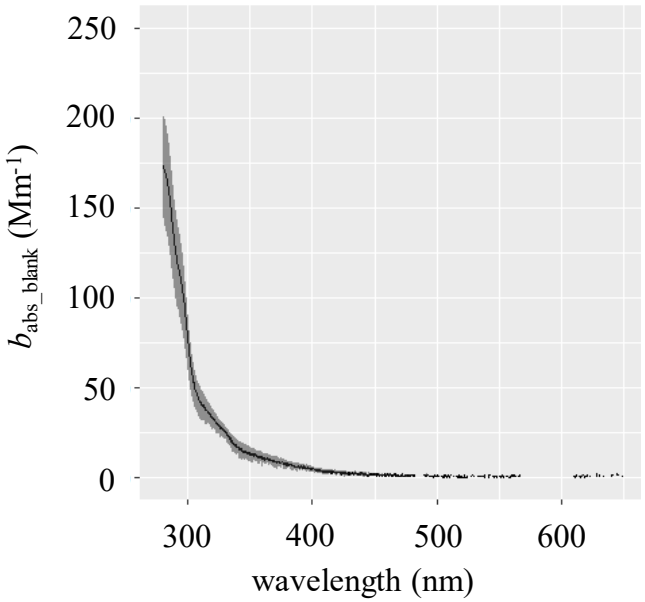

143

144 **Figure S4.** The absorption coefficient of blanks ($b_{abs–blank}$, Mm^{-1}) in methanol extracts. The
145 black line in the middle is averaged blank (mean) from the blank filters collected from the
146 cleaned chamber and from the control experiments (see sampling information of blank
147 filters in Table S2). The upper limit of shaded area is mean + SD, the lower limit is mean
148 − SD.

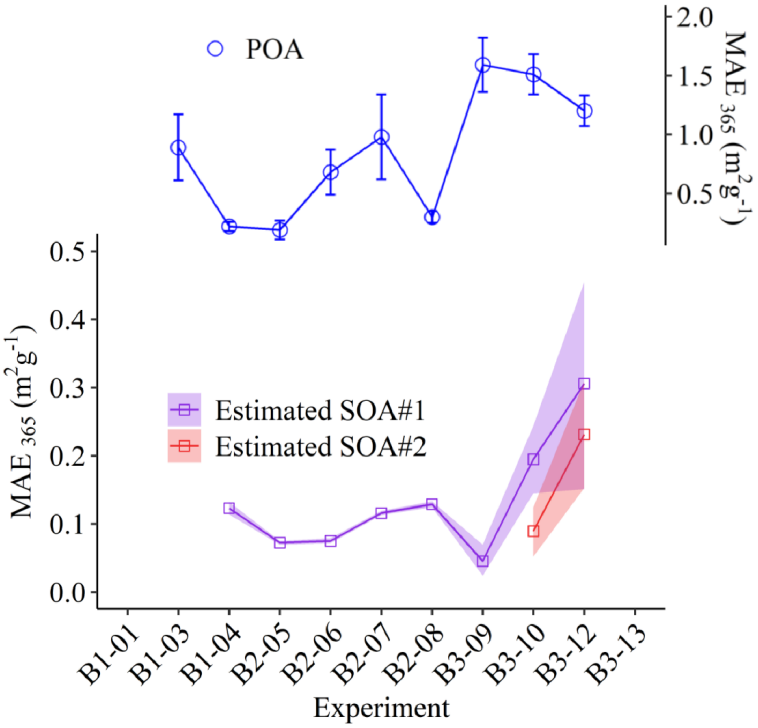

Figure S5. The MAE at 365 nm for the SOA estimated according to eq 6 with the assumption that the MAE_{POA} is constant during the aging experiment (square symbols). If the MAE_{POA} changes within ± 20% during aging relative to the MAE_{POA} determined before aging, then the estimated MAE_{SOA} will also change in the range indicated using the shaded areas. For experiments B3-10 and B3-12, two filters (i.e., #1 and #2) were collected after UV lights on (aging starts). The measured MAE values at 365 nm for POA are also shown for comparison.

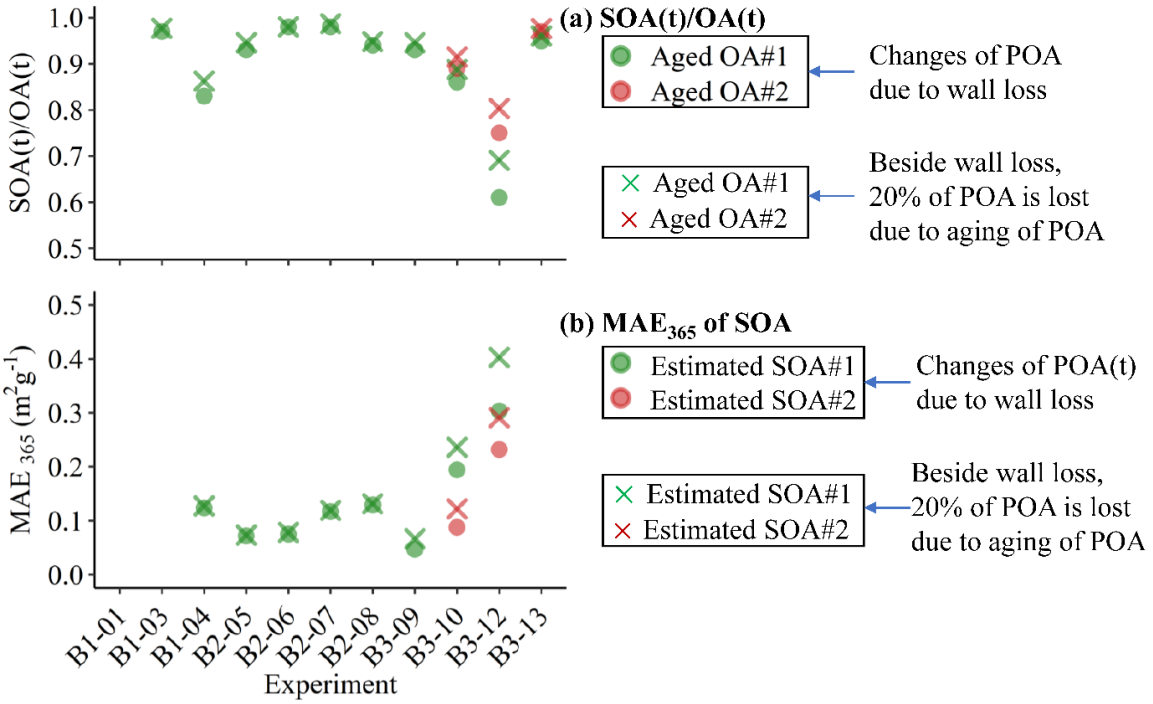

157

158 **Figure S6. (a)** Proportion of SOA in the aged OA (SOA(t)/OA(t)) and **(b)** the MAE at 365
159 nm for SOA, under the assumption that changes of POA concentrations are exclusively due
160 to wall losses, or under the assumption that besides wall loss, 20% of POA mass is lost due
161 to aging of POA. t is the time period when the aged aerosols were collected. For
162 experiments B3-10, B3-12 and B3-13, two filters (i.e., #1 and #2) were collected after UV
163 lights on (aging starts).

Table S1. Coal properties by proximate and ultimate analysis[a].

Type	**Anthracite**		**Bituminous**		
	Clean coal #1	Clean coal #2	Dirty coal#1	Dirty coal#2	Dirty coal#3
Coal ID	A1	A2	B1	B2	B3
Proximate analysis (wt%)					
Moisture[*]	0.88	1.18	9.04	8.31	0.46
Ash[**]	9.42	6.06	4.79	4.89	25.12
Volatile matter[***]	6.85	8.28	29.7	33.11	28.49
Fixed carbon[*]	83.28	85.04	60.51	57.69	53.15
Ultimate analysis (wt%)[**]					
C	78.89	84.31	67.9	60.15	64.26
H	2.48	3.28	3.11	2.88	3.4
O	0.91	0.76	0.72	0.8	1.03
N	3.82	3.46	12.48	13.5	5.01
S	0.57	0.34	0.11	0.18	0.38
Lower heating value ($MJ\ kg^{-1}$)[**]	29.68	32.33	25.38	22.08	24.93

[a]Measured by Shaanxi Coal Geological Laboratory Co., Ltd., China on the basis of the national standards of the People's Republic of China (GB/T 212-2008, GB/T213-2008, GB/T476-2008, GB/T19227-2008, GB/T476-2001).

[*]based on air-dry basis; [**] as received; [***] volatile matter on dry and ash-free basis.

Table S2. Summary of filter samples from primary and aged emissions for UV–visible measurements.

Experiment	Blank[a]	Primary[b]	Aged[c]	Coal ID[d]	Weight of Coal (g)	Oven Temp. in pre-heated chamber (°C)[e]
B1-01	**1**[f]	1	1	B1	200	600
B1-02	/	1	1	B1	203	660
B1-03	/	1	1	B1	202	650
B1-04	**1**[f]	1	1	B1	203	650
B2-05	/	1	1	B2	203	630
B2-06	/	1	1	B2	202	650
B2-07	/	1	1	B2	201	650
B2-08	/	1	1	B2	205	640
B3-09	/	1	1	B3	200	650
B3-10	/	1	2	B3	200	630
B3-12	/	1	2	B3	208	650
B3-13	/	1	2	B3	206	610
A2-14	/	1	1	A2	289	630
A1-16	/	1	1	A1	200	650
control experiment	/	/	**1**[f]		no emission injection	
control experiment	/	/	**1**[f]		no emission injection	

[a] Blank filters collected from cleaned chamber, prior to injection of coal exhausts.
[b] Filters collected primary particles from smog chamber before UV lights on.
[c] Filters collected aged particles from smog chamber. For some experiments we collected two filters after UV lights on (aging starts).
[d] Coal ID was described in Table S1.
[e] Temperature in the preheated combustion chamber of the stove before adding the sample coal, monitored with a thermocouple probe situated closely above the coal.
[f] Used for blank corrections. See details in Text S4 and FigureS4.

Table S3. Methanol-extracted MAE_{365} of primary and aged emissions from each experiment of coal, with the OA loading on the filter samples (M_{OA}), C_{OA} during the filter sampling, f_{OA} for the primary emissions (i.e., an indicator of combustion conditions) during the filter sampling, and OH exposure as an indicator of aging in this study.

Expt[a]	Filter samples	M_{OA} [b] (integrated, μg)	C_{OA} [b] (μg m^{-3})	MAE_{365} (m^2 g^{-1})[c]	f_{OA} (primary)	OH exposure ($\times10^7$, molec cm^{-3} h)
B1-01	primary	/	/	/	/	0
B1-03	primary	0.38 ± 0.04	11.9 ± 1.39	0.89 ± 0.28	0.37	0
B1-04	primary	9.05 ± 1.04	217.9 ± 25.0	0.22 ± 0.04	0.85	0
B2-05	primary	1.63 ± 0.22	39.2 ± 5.4	0.19 ± 0.08	0.82	0
B2-06	primary	1.19 ± 0.28	42.9 ± 10.2	0.68 ± 0.19	0.84	0
B2-07	primary	1.52 ± 0.51	27.4 ± 9.2	0.98 ± 0.36	0.54	0
B2-08	primary	4.81 ± 0.45	117.6 ± 11.1	0.30 ± 0.05	0.84	0
B3-09	primary	1.32 ± 0.10	27.8 ± 2.0	1.59 ± 0.23	0.04	0
B3-10	primary	9.09 ± 0.42	291.2 ± 13.3	1.51 ± 0.17	/	0
B3-12	primary	12.24 ± 0.59	441.7 ± 21.1	1.20 ± 0.13	0.10	0
B3-13	primary	1.14 ± 0.34	20.6 ± 6.1	NA[d]	/	0
B1-01	aged	18.41 ± 0.71	553.8 ± 21.2	0.13 ± 0.02		2.18 ± 0.18
B1-03	aged	6.26 ± 0.17	96.0 ± 2.5	NA[d]		5.66 ± 0.35
B1-04	aged	18.31 ± 0.71	440.7 ± 17.0	0.14 ± 0.02		3.54 ± 0.19
B2-05	aged	8.02 ± 0.08	193.0 ± 1.9	0.08 ± 0.02		4.25 ± 0.15
B2-06	aged	10.13 ± 0.21	243.7 ± 5.1	0.09 ± 0.02		4.50 ± 0.15
B2-07	aged	12.73 ± 0.17	306.4 ± 4.1	0.13 ± 0.02		3.20 ± 0.15
B2-08	aged	14.02 ± 0.39	339.1 ± 9.5	0.14 ± 0.02		3.48 ± 0.14
B3-09	aged	2.14 ± 0.04	52.2 ± 1.1	0.15 ± 0.06		6.42 ± 0.22
B3-10	aged#1	16.44 ± 0.28	395.7 ± 6.7	0.38 ± 0.04		3.69 ± 0.10
B3-12	aged#1	8.16 ± 0.24	298.9 ± 8.7	0.65 ± 0.07		3.24 ± 0.11
B3-13	aged#1	7.79 ± 0.30	137.8 ± 5.2	NA[d]		6.08 ± 2.78
B3-10	aged#2	16.90 ± 0.27	406.8 ± 6.4	0.24 ± 0.03		4.32 ± 0.71
B3-12	aged#2	7.13 ± 0.16	257.4 ± 5.8	0.47 ± 0.05		4.83 ± 0.16
B3-13	aged#2	6.77 ± 0.03	161.2 ± 0.6	NA[d]		8.09 ± 1.76

[a] Experiment number see details in Table S2.
[b] Absolute uncertainties are given.
[c] Calculation of uncertainties for MAE is described in Text S5.
[d] b_{abs} of the sample is smaller than the blank signals. See the blank signals in Figure S4.

Table S4. Averaged MAE_{365} of methanol extracts from residential coal combustion emissions.

Coal type	MAE_{365} (m^2 g^{-1})	
	Primary	Aged
B1	0.56 (0.22–0.89)[a] (n=2)[b]	0.14 (0.13–0.14) (n=2)[b]
B2	0.54 ± 0.36 (0.19–0.98) (n=4)	0.11 ± 0.03 (0.08–0.14) (n=4)
B3	1.43 ± 0.21 (1.20–1.59) (n=3)	0.38 ± 0.20 (0.15–0.65) (n=5)[c]
Average	0.84 ± 0.54 (n=9)	0.24 ± 0.18 (n=11)[c]

[a] The average and minimum-maximum range.

[b] For n<2, only average values are given. For n>3, average ± SD are given.

[c] Including both aged#1 and aged#2 (see Table S3 for sample information).

References

(1) Zhi, G.; Chen, Y.; Feng, Y.; Xiong, S.; Li, J.; Zhang, G.; Sheng, G.; Fu, J. Emission characteristics of carbonaceous particles from various residential coal-stoves in China. *Environ. Sci. Technol.* **2008**, *42* (9), 3310-3315.

(2) Bertrand, A.; Stefenelli, G.; Bruns, E. A.; Pieber, S. M.; Temime-Roussel, B.; Slowik, J. G.; Prévôt, A. S. H.; Wortham, H.; El Haddad, I.; Marchand, N. Primary emissions and secondary aerosol production potential from woodstoves for residential heating: Influence of the stove technology and combustion efficiency. *Atmos. Environ.* **2017**, *169*, 65-79.

(3) Bruns, E.; Krapf, M.; Orasche, J.; Huang, Y.; Zimmermann, R.; Drinovec, L.; Močnik, G.; El-Haddad, I.; Slowik, J.; Dommen, J. Characterization of primary and secondary wood combustion products generated under different burner loads. *Atmos. Chem. Phys.* **2015**, *15* (5), 2825-2841.

(4) Bruns, E. A.; El Haddad, I.; Slowik, J. G.; Kilic, D.; Klein, F.; Baltensperger, U.; Prévôt, A. S. Identification of significant precursor gases of secondary organic aerosols from residential wood combustion. *Sci Rep*. **2016**, *6*, 27881.

(5) Platt, S. M.; El Haddad, I.; Zardini, A. A.; Clairotte, M.; Astorga, C.; Wolf, R.; Slowik, J. G.; Temime-Roussel, B.; Marchand, N.; Ježek, I.; Drinovec, L.; Močnik, G.; Möhler, O.; Richter, R.; Barmet, P.; Bianchi, F.; Baltensperger, U.; Prévôt, A. S. H. Secondary organic aerosol formation from gasoline vehicle emissions in a new mobile environmental reaction chamber. *Atmos. Chem. Phys.* **2013**, *13* (18), 9141-9158.

(6) Drinovec, L.; Močnik, G.; Zotter, P.; Prévôt, A.; Ruckstuhl, C.; Coz, E.; Rupakheti, M.; Sciare, J.; Müller, T.; Wiedensohler, A. The "dual-spot" Aethalometer: An improved measurement of aerosol black carbon with real-time loading compensation. *Atmos. Meas. Tech.* **2015**, *8* (5), 1965.

(7) Daellenbach, K.; Bozzetti, C.; Křepelová, A.; Canonaco, F.; Wolf, R.; Zotter, P.; Fermo, P.; Crippa, M.; Slowik, J.; Sosedova, Y. Characterization and source apportionment of organic aerosol using offline aerosol mass spectrometry. *Atmos. Meas. Tech.* **2016**, *9* (1), 23-39.

(8) Krapf, M.; El Haddad, I.; Bruns, Emily A.; Molteni, U.; Daellenbach, Kaspar R.; Prévôt, André S. H.; Baltensperger, U.; Dommen, J. Labile peroxides in secondary organic aerosol. *Chem* **2016**, *1* (4), 603-616.

(9) Kumar, N. K.; Corbin, J. C.; Bruns, E. A.; Massabó, D.; Slowik, J. G.; Drinovec, L.; Močnik, G.; Prati, P.; Vlachou, A.; Baltensperger, U.; Gysel, M.; El-Haddad, I.; Prévôt, A. S. H. Production of particulate brown carbon during atmospheric aging of residential wood-burning emissions. *Atmos. Chem. Phys.* **2018**, *18* (24), 17843-17861.

(10) Moschos, V.; Kumar, N. K.; Daellenbach, K. R.; Baltensperger, U.; Prévôt, A. S.; El Haddad, I. Source apportionment of brown carbon absorption by coupling UV/Vis spectroscopy with aerosol mass spectrometry. *Environ. Sci. Technol. Lett.* **2018**, *5* (6), 302-308.

(11) Rocke, D. M.; Lorenzato, S. A two-component model for measurement error in analytical chemistry. *Technometrics* **1995**, *37* (2), 176-184.

(12) Wilson, M. D.; Rocke, D. M.; Durbin, B.; Kahn, H. D. Detection limits and goodness-of-fit measures for the two-component model of chemical analytical error. *Anal. Chim. Acta* **2004**, *509* (2), 197-208.